Am J Transl Res 2025;17(4):3109-3118
www.ajtr.org /ISSN:1943-8141/AJTR0161304

Original Article

Correlation between ultrasound measurements and the expression of Her-2 and CD147 in breast cancer

Ping He[1], Lei Zhang[1], Fengwei Zhu[2], Jing Zhao[1], Yue Liu[1], Huabin Zhang[1]

[1]Department of Ultrasound, Beijing Tsinghua Changgung Hospital, School of Clinical Medicine, Tsinghua University, Beijing 102218, PR China; [2]The First Medical Center, Chinese PLA General Hospital and PLA Medical School, Beijing 100853, PR China

Received October 18, 2024; Accepted April 7, 2025; Epub April 15, 2025; Published April 30, 2025

Abstract: Objective: To analyze the correlation between ultrasound data and Her-2 and CD147 expressions in breast carcinoma. Method: A retrospective analysis was conducted on 95 patients with invasive breast carcinoma, hospitalized during March 2021 to May 2024, designated as the breast cancer group. Additionally, 80 cases with benign breast lesions were selected as the control group. Contrast-enhanced ultrasound (CEUS) was performed on both groups. Immunohistochemistry was used to detect the expression of Her-2 and CD147 proteins in breast cancer and adjacent tissues, while RT-qPCR was employed to measure the mRNA expression of Her-2 and CD147 in the cancer and adjacent tissues. Results: The peak time in the breast cancer group was shorter than in the control group (P<0.05). Conversely, the enhancement amplitude, slope of ascending branch, area under the curve, and gradient were higher in the breast cancer group than in the control group (all P<0.05). There was a significant negative correlation between peak time of ultrasound parameters and the relative expression of Her-2 and CD147 mRNA (P<0.05). In contrast, the enhancement amplitude, slope of the ascending branch, area under the curve, and gradient exhibited positive correlations with the relative expression of Her-2 and CD147 mRNA in cancer tissues (P<0.05). Conclusion: The contrast-enhanced ultrasound data of malignant breast tumors significantly differed from those of benign tumors, demonstrating good diagnostic value for breast cancer. In addition, these ultrasound data were significantly correlated with the expression of Her-2 and CD147 in tumor tissues, providing valuable insight for the non-invasive assessment of early-stage breast cancer and offering a reference for diagnosis and treatment planning.

Keywords: Breast cancer, ultrasonic parameters, Her-2, CD147, correlation

Introduction

Breast cancer is a malignacy characterized by the uncontrolled proliferation of breast epithelial cells, driven by multiple carcinogenic factors. It is the most frequently diagnosed malignancy in women, ranking first in incidence among female-specific cancers [1]. Most breast cancer patients do not exhibit obvious symptoms; however, some may present with a breast lump or nipple discharge. As the disease progresses, patients may experience lymph node and distant metastasis, significantly affecting survival [2]. In recent years, the incidence of breast cancer in China has steadily increased. Although treatment protocols for breast cancer have gradually matured, resulting in better overall control of patient mortality rates, the mortality rate remains high in economically underdeveloped regions. Consequently, improving treatment and prognosis remains a critical focus for clinical practitioners [3, 4].

Color Doppler ultrasound (CDU) plays a crucial role in the diagnosis of breast cancer, particularly in distinguishing benign from malignant tumors. It provides essential guidance for clinical diagnosis and treatment planning. However, standalone ultrasound still carries a certain risk of missed diagnoses [5]. Recently, the combination of breast cancer imaging technology and pathology has gained popularity in clinical practice. By incorporating biological markers and immunological technologies, researchers are studying the molecular characteristics of breast cancer to better understand its development and treatment [6].

https://doi.org/10.62347/JAVK7987

As a proto-oncogene, human epidermal growth factor receptor 2 (Her-2) plays a crucial role in regulating cell growth, proliferation, and survival. Overexpression of Her-2 is closely associated with the invasiveness of breast cancer, an increased risk of lymph node metastasis, and poor prognosis. Tumor cells in Her-2-positive patients exhibit high proliferation activity, a tendency for distant metastasis (e.g., to the liver and lungs), and reduced sensitivity to conventional chemotherapy [7, 8]. CD147 is a cell surface glycoprotein and a member of the immunoglobulin superfamily. It acts as an inducer of matrix metalloproteinases (MMPs) on tumor cell surface, promoting the release of MMPs. This process facilitates the degradation of the extracellular matrix and basement membrane, thereby facilitating tumor cell infiltration and metastasis. CD147 promotes tumor angiogenesis, invasion, and metastasis by inducing the release of MMPs and degrading the extracellular matrix [9]. Breast cancer patients with high CD147 expression are more likely to experience axillary lymph node metastasis and have a significantly lower 5-year survival rate [10]. To enhance the practical value of ultrasound in breast cancer diagnosis and investigate the relationship between ultrasound data and tumor pathologic characteristics, this study explored the correlation between ultrasound data and Her-2 and CD147 expression in breast cancer.

Materials and methods

Clinical data

This retrospective study enrolled 95 patients with invasive breast cancer who were hospitalized between March 2021 and May 2024, designated as the breast cancer group. Additionally, 80 cases of benign breast tumor were selected as control group. The study was approved by the Ethics Committee of Beijing Tsinghua Changgung Hospital. Sample size calculation for both groups was based on the formula $N = Z^2 * \sigma^2/d^2$, where Z is the critical value of the standard normal distribution corresponding to the confidence level ($Z = 1.96$ when $\alpha = 0.05$), σ is the estimated overall standard deviation (based on previous studies or pilot experiments), and d is the maximum allowable difference between the sample mean and the overall mean. According to previous literature, the maximum tumor diameter was used as the primary observation index. For the breast cancer group: $\sigma = 1.8$ cm (based on the dispersion of tumor diameters in invasive breast cancer), $d = 0.4$ cm, $N = (1.96^2 \times 1.8^2)/0.4^2 \approx 77$; For the control group: $\sigma = 1.5$ cm (based on the variation in benign tumor diameters), $d = 0.4$ cm, $N = (1.96^2 \times 1.5^2)/0.4^2 \approx 55$. Additionally, the sample size was appropriately increased based on the number of patients that could be included in the hospital during the same period to enhance statistical power.

Inclusion and exclusion criteria

Inclusion criteria: (1) Patients with breast carcinoma diagnosed according to the Chinese Anti-Cancer Association guidelines for invasive breast cancer and the 2015 guidelines for the diagnosis and treatment of breast cancer [11], confirmed by pathology examination; (2) Patients in the control group who met the diagnostic criteria for benign breast tumors as outlined in modern diagnostic and therapeutic science of breast hyperplasia and benign tumor [12]; (3) Patients had unilateral primary tumors; (4) Both groups underwent surgical treatment and had ultrasound examination before operation.

Exclusion criteria: (1) Patients with concomitant primary malignant tumors; (2) Patients with severe organic disease; (3) Patients with a history of chest surgery; (4) Patients with contraindications to ultrasound examination; or (5) Pregnant or lactating women.

Methods

Ultrasonic examination: The standardization of the examination process followed the “Chinese Expert Consensus on the Clinical Application of Venous Contrast-Enhanced Ultrasound in Gynecological and Obstetric Diseases (2023 Edition) [13]”. Both groups underwent contrast-enhanced ultrasound using Siemens s3000 ultrasound diagnostic equipment (Germany), with a probe frequency of 9-15 MHz, and the Snon Vue contrast agent (Bracco, Italy). During the examination, patients were positioned supine with their arms raised to expose the breast. The lesions were observed using conventional polytangent surfaces. Once the ultrasound image clearly showed the lesion, the system was switched to contrast mode. The dynamic perfusion process and enhancement patterns of the lesions were observed for 3-5

minutes after the injection of 2.4 ml contrast medium and 5 ml normal saline. The images were analyzed using QLAB software.

Four areas of interest (upper, lower, left, and right) were selected at the edge of the enhancement zone of the lesion. Care was taken to avoid areas near nourishing vessels or necrotic vascular regions. Time-intensity curves for each region were automatically generated by QLAB. Perfusion parameters, including peak time, enhancement amplitude, inclination of ascending branch, area under de-line, and gradient, were obtained after curve fitting. The images were independently reviewed by two experienced sonographers, blinded to the clinical outcomes.

Immunohistochemical detection: Cancerous and adjacent tissues were embedded in paraffin, then sectioned into 4 μm thick slices for immunohistochemical staining. The EnVision method was adopted with color development achieved through DAB. The immunohistochemical detection kit was procured from Beijing Zhongshanjinqiao Biotechnology Co., Ltd., and Her-2 and CD147 antibodies were purchased from ABCAM company.

Two pathologists independently reviewed the slides using a double-blind method, assessing staining intensity and the percentage of positive stained cells. The staining intensity was scored as follows [14]: no staining (0), light brown (1), brownish yellow (2), dark brown (3). The percentage of positive cells was scored as follows: <25% (1), 25%-50% (2), and >50% (3). The final score for each sample was calculated by multiplying the staining intensity score by the percentage score. A weighted score of 0 was considered negative, while all other scores were considered positive.

RT-qPCR detection: Total RNA was extracted from cancer tissue and adjacent tissues by Trizol method, and its concentration and purity were examined. RNA was then reverse-transcribed into cDNA with primers designed using Primer 5.0 software. The primer sequence was synthesized by Shanghai Shenggong Bioengineering Co., LTD. Primer sequence: Her-2: upstream primer 5'-TGCTGTCCTGTTCACCACTC-3', downstream primer 5'-tcatcctcatcTTcacattg-3'; CD147: Upstream primer: 5'-GACTCCGACGACC AGTGGGGAGAGTACTCCTGGGT-3', downstream primer: 5'-GAACATGGAGGCCGACCC CGGCCAG-TACCGGTGCA-3'; β-catin: upstream primer 5'-GTCTTCCCCTCCA TCGTG-3', downstream primer 5'-AGGGTGAGGATGCCTCTC-3'. Reaction conditions were 94°C for 4 minutes, 94°C for 20 seconds, 60°C for 30 seconds, and 72°C for 30 seconds, completing a total of 35 rounds. Using β-actin as internal reference gene, the relative expression of target gene was expressed as $2^{-\Delta\Delta Ct}$.

Statistical analysis

SPSS 27.0 was adopted for data processing and analysis. The t-test was used for the comparison of continuous variables and χ^2 test was performed for the comparison of categorical data. The diagnostic value of ultrasound parameters for breast cancer was assessed using receiver operating characteristic (ROC) curves, and correlation analysis was performed using Pearson's correlation. A *P*-value of <0.05 was considered significant.

Results

Comparison of baseline data of the two groups

The age of patients in the breast cancer group was (50.12±5.36) years, BMI was (23.18±2.96) kg/m^2, the average number of deliveries was (1.26±0.25) times, and the maximum diameter of the tumor was (1.89±0.51) cm. In the control group, the age was (49.83±6.03) years old, BMI was (23.25±2.87) kg/m^2, the average number of deliveries was (1.29±0.30) times, and the maximum tumor diameter was (1.75±0.49) cm. No significant differences were observed in age, BMI, parity, or tumor diameter between the two groups (all *P>0.05*) (**Table 1**). A typical case is shown in **Figure 1**.

Comparison of ultrasound data between two groups

In the breast cancer group, the peak time was (21.56±5.47) s, the enhancement amplitude was (6.52±2.31) dB, the ascending slope was (14.94±3.42), the area under the curve was (453.94±126.34), and the gradient was (1.18±0.42). The peak time of patients in the control group was (25.29±4.98) s, the enhancement amplitude was (4.38±1.34) dB, the as-

Table 1. Comparison of baseline data between the two groups ($\bar{x}\pm s$)

Clinical data	Breast cancer group (n = 95)	Control group (n = 80)	t/x^2	*P*
Age (yrs, $\bar{x}\pm s$)	50.12±5.36	49.83±6.03	0.337	0.737
BMI (kg/m^2, $\bar{x}\pm s$)	23.18±2.96	23.25±2.87	0.158	0.875
Production times (times, $\bar{x}\pm s$)	1.26±0.25	1.29±0.30	0.272	0.472
Maximum tumor diameter(cm, $\bar{x}\pm s$)	1.89±0.51	1.75±0.49	1.842	0.067
Hypertension (n, %)	10 (10.53)	7 (8.75)	0.156	0.693
Diabetes (n,%)	6 (6.32)	7 (8.75)	0.374	0.541

BMI: body mass index.

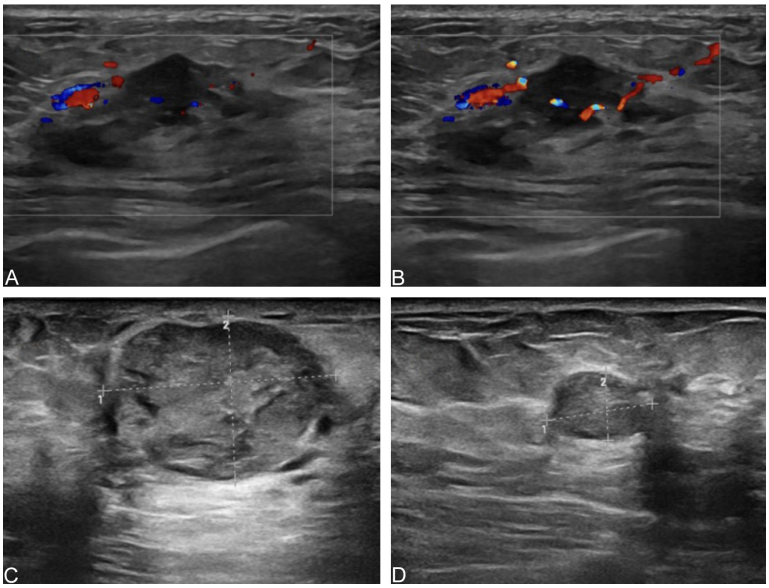

Figure 1. Typical case ultrasound image. A, B: A 58-year-old female with a right breast biopsy showing three fine thread-like tissues, grayish-white and grayish-yellow in color, measuring 0.8-1 cm in length and 0.1 cm in diameter. The biopsy was confirmed as invasive breast cancer. The contrast-enhanced ultrasound of the patient revealed a peak time of 18.48 seconds, enhancement amplitude of 5.98 dB, ascending slope of 15.22, area under the curve of 469.45, and a gradient of 1.09. Both Her-2 and CD147 expressions in the cancer tissue were positive. C, D: A 71-year-old female with a left breast mass measuring 24 × 21 × 5 cm. No abnormalities were observed on the skin surface or nipple. The clinical incision site revealed a mass of 3.5 × 3.5 × 2.5 cm, containing a significant amount of mucus and soft in texture. The mass was adjacent to the skin and nipple, approximately 3 cm from the resection margin. The remaining breast tissue was grayish-white and grayish-yellow with soft texture. The mass was confirmed as solid papillary carcinoma with invasion. The contrast-enhanced ultrasound of the patient revealed a peak time of 19.34 seconds, enhancement amplitude of 7.38 dB, ascending slope of 12.94, area under the curve of 419.38, and a gradient of 1.30. Both Her-2 and CD147 expressions in the cancer tissue were positive.

cending slope was (8.30±2.93), the area under the curve was (332.38±101.93), and the gradient was (0.73±0.21). The peak time in breast cancer group was shorter than in the control group (*P<0.05*), and the enhancement amplitude, ascending slope, area under the curve, and gradient were all significantly higher in the breast cancer group compared to the control group (all *P<0.05*) (**Table 2**).

Diagnostic value of ultrasound data in breast cancer

The diagnostic value of ultrasound parameters for breast cancer was assessed using ROC curve analysis. The results revealed that the peak time, enhancement amplitude, ascending slope, area under the curve and the gradient were achieved AUCs of 0.692, 0.789, 0.929, 0.772, and 0.831 (**Figure 2**; **Table 3**).

Comparison of positive rate of Her-2 and CD147 expression in different tissues

The positive rate of Her-2 expression was 76.84% in breast cancer tissues and 10.53% in para-cancer tissues. The positive rate of CD147 expression was 89.95% in breast cancer tissues and 13.68% in adjacent tissues. The positive rates of Her-2 and CD147 in breast cancer tissues were apparently higher than those in adjacent tissues (*P<0.05*) (**Table 4**; **Figure 3**).

Comparison of Her-2 and CD147 mRNA expression in two different tissues

The relative mRNA expression of Her-2 and CD147 was significantly higher in breast cancer tissues compared to adjacent tissues (both *P<0.05*, **Table 5**).

Table 2. Comparison of ultrasound data between the two groups (x±s)

Indicator	Breast cancer group (n = 95)	Control Group (n = 80)	t	*P*
Peak time (s)	21.56±5.47	25.29±4.98	4.680	0.000
Enhancement amplitude (dB)	6.52±2.31	4.38±1.34	7.313	0.000
Slope of ascending branch	14.94±3.42	8.30±2.93	13.651	0.000
Area under the curve	453.94±126.34	332.38±101.93	6.916	0.000
Gradient	1.18±0.42	0.73±0.21	8.708	0.000

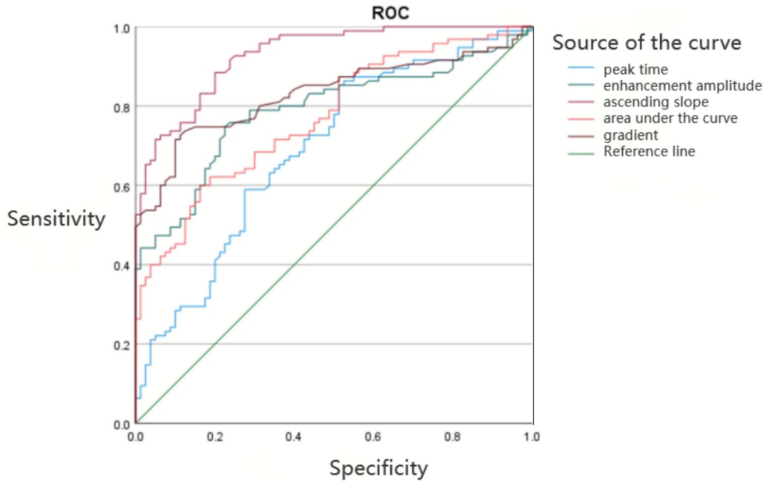

Figure 2. ROC curve analysis of ultrasound parameters for the diagnosis of breast cancer.

Correlation analysis of ultrasound data and expression of Her-2 and CD147 mRNA in breast cancer

A significant negative correlation was observed between the peak time of ultrasound data and the relative expression of Her-2 and CD147 mRNA (*P<0.05*). In contrast, the ultrasound data of enhancement amplitude, slope of ascending branch, area under the curve, and gradient were significantly positively correlated with the relative expression of Her-2 and CD147 mRNA in cancer tissues (*P<0.05*) (**Table 6**; **Figure 4**).

Discussion

The occurrence and progression of breast cancer are closely linked to tumor angiogenesis. In the peritumoral region, where cancer cells exhibit heightened proliferative activity, a dense network of blood vessels is formed. Microvessels in this area also anastomose, forming complex loops [15, 16]. Contrast-enhanced ultrasound (CEUS), the most commonly used imaging technique, provides valuable morphologic information for diagnosing malignant tumors. In addition, the contrast agent, acting as a tracer of blood pool, reveals the temporal sequence and spatial distribution of microvascular perfusion in organs and tissues, highlighting their differences. CEUS reflects organ and tumor perfusion from the perspective of microcirculation, aiding hemodynamic studies and providing critical information for diagnosing malignant tumors and predicting patient prognosis [17-19]. The peak time reflects the point at which the contrast agent reaches its peak diffusion and serves as an indicator of blood vessel patency and collateral circulation capability. A shorter peak time suggests more abundant blood vessels within the tumor and a higher likelihood of malignancy. Therefore, breast cancer patients show a significant reduction in peak time [20, 21]. In addition, the enhancement amplitude, ascending slope, area under the curve, and gradient in the breast cancer group are significantly increased, reflecting the malignant proliferation of tumor cells. These findings are consistent with the results of related studies [22-24].

Her-2, a member of human epidermal growth factor receptor family, is located on the q21 region of chromosome 17 and is a reamer protein with tyrosine kinase activity [25, 26]. Her-2 monomers are not activated under normal physiologic conditions. Upon phosphorylation, the tyrosine residues in Her-2 monomers mediate intracellular phosphorylation, gene expression, and DNA synthesis [27, 28]. In a pathological state, overexpression of Her-2 on the cell membrane can drive rapid cellular proliferation and tumor formation, playing a critical role in both tumorigenesis and tumor progression [29]. CD147, a member of immunoglobulin

Table 3. Diagnostic value of ultrasound parameters in breast cancer analyzed using ROC curve

Indicator	Area under the curve	Truncation value	Sensitivity	Specificity	*P*	95% CI
Peak time	0.692	22.654 s	85.30%	48.70%	0.000	0.613-0.770
Enhancement amplitude	0.789	5.275 dB	74.70%	77.50%	0.000	0.721-0.857
Ascending slope	0.929	11.075	88.40%	80.00%	0.000	0.895-0.964
Area under the curve	0.772	429.15	60.00%	83.80%	0.000	0.704-0.840
Gradient	0.831	0.995	71.60%	90.00%	0.000	0.769-0.893

ROC: receiver operating characteristic.

Table 4. Comparison of positive rate of Her-2 and CD147 expression between two groups [n (%)]

Expression	Breast cancer group (n = 95)	Control Group (n = 80)	x^2	*P*
Her-2				
Positive	73 (76.84)	10 (10.53)	84.913	0.000
Negative	22 (23.16)	85 (89.47)		
CD147				
Positive	75 (89.95)	13 (13.68)	81.368	0.000
Negative	20 (21.05)	82 (86.32)		

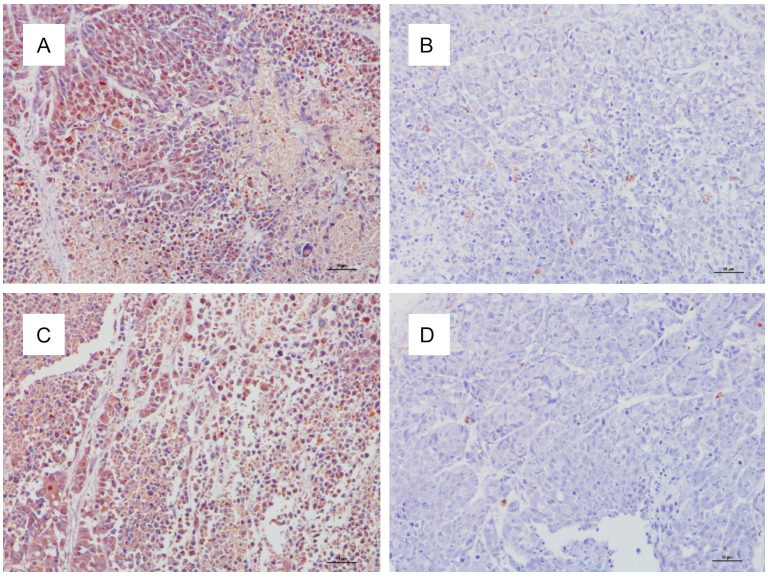

Figure 3. Positive expression of Her-2 and CD147 in breast cancer tissues. A: Positive expression of Her-2 in cancer tissue; B: Negative expression of Her-2 in cancer tissue; C: Positive expression of CD147 in cancer tissue; D: Negative expression of CD147 in cancer tissue.

family, is expressed on the surface of tumor cells. CD147 stimulates the synthesis of MMPs by fibroblasts near tumors, thus promoting tumor cell invasion and metastasis [30-32]. Studies have shown that the positive expression rates of Her-2 and CD147 proteins in breast cancer tissues are apparently higher than those in adjacent tissues. Additionally, relative mRNA expression of Her-2 and CD147 was higher in breast cancer tissues than those of adjacent tissues. This suggests that Her-2 and CD147 expression may be associated with the onset and progression of breast cancer.

To further confirm the diagnostic value of contrast-enhanced ultrasound and its relationship with Her-2 and CD147 expression in tumortissue, this study analyzed the correlation between ultrasound data of breast cancer and the expression of Her-2 and CD147. The results demonstrated that the peak time in the breast cancer group was remarkably shorter than that in control group. Additionally, the enhancement amplitude, slope of ascending branch, area under the curve, and gradient were significantly higher in the breast cancer group compared to the control group. These findings are consistent with previous research, which reported similar results [33-35], indicating the high perfusion characteristics of neovascularization in malignant tumors. The contrast-enhanced ultrasound parameters exhibit significant differences between breast cancer

Table 5. Comparison of Her-2 and CD147 mRNA expression between the two groups ($\bar{x}\pm s$)

Index	Breast cancer group (n = 95)	Control Group (n = 80)	t	*P*
Her-2	1.894±0.364	1.037±0.262	18.625	0.000
CD147	1.695±0.283	0.997±0.169	20.640	0.000

Table 6. Correlation analysis between ultrasound parameters and mRNA expression of Her-2 and CD147 in cancer tissues

Indicator	Statistical value	Peak time	Enhancement amplitude	Slope of ascending branch	Area under the curve	Gradient
Her-2	r	-0.472	0.522	0.498	0.536	0.510
	P	0.000	0.000	0.000	0.000	0.000
CD147	r	-0.459	0.558	0.503	0.483	0.529
	P	0.000	0.000	0.000	0.000	0.000

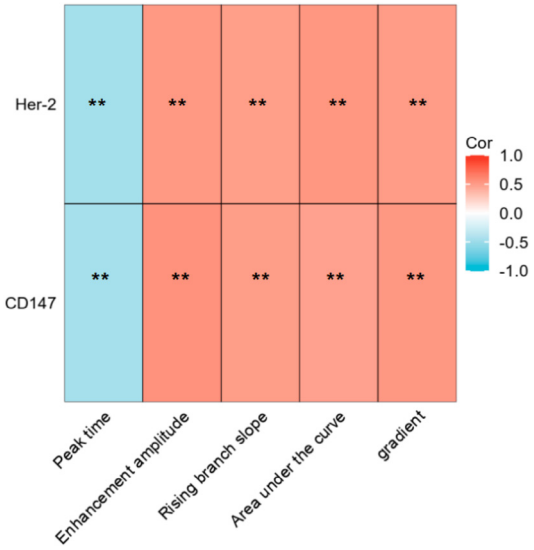

Figure 4. Correlation analysis heat map. **P<0.001.

and benign breast tumors, providing important diagnostic value for the diagnosis of breast cancer.

The correlation analysis showed a significant negative correlation between the peak time of ultrasound data and the relative expression of Her-2 and CD147 mRNA in breast cancer tissues. Conversely, the ultrasound measurements of enhancement amplitude, slope of ascending branch, area under the curve, and gradient were significantly positively correlated with the relative expression of Her-2 and CD147 mRNA. These results indicate a strong correlation between the protein expression in breast cancer tissues and contrast-enhanced ultrasound parameters. This finding suggests that contrast-enhanced ultrasound parameters may serve as a non-invasive alternative to histologic examination for early assessment of breast cancer, offering valuable references for clinical diagnosis and treatment. These results may involve Her-2 overexpression, which promotes the proliferation of tumor vascular endothelial cells by activating the PI3K/AKT signaling pathway. This accelerates contrast agent perfusion in newly formed blood vessels, thereby shortening the peak time and enhancing early enhancement intensity. CD147, on the other hand, increases the microvascular permeability by up-regulating MMPs, which disrupt the integrity of the basement membrane, resulting in prolonged contrast agent retention and an elevated area under the curve value.

This study is the first to analyze jointly the correlation between ultrasound parameters of breast cancer and dual biomarkers, Her-2 and CD147, filling the gap in research on the association between CD147 (a key transmembrane glycoprotein that regulates tumor invasion and metastasis) and ultrasound features. However, this study has limitations due to the relatively small sample size, which may affect the stability of the statistical model and limit the depth of subgroup analysis, such as the interaction between Her-2-positive and CD147-high expression subgroups. A small sample size also restricts the adjustment for confounding factors (e.g., age, molecular typing, and underlying diseases), affecting the precise quantification of the correlation between ultrasound data and molecular markers. To address these limitations, future research will adopt a multi-center collaborative approach with expanded sample

size. Stratified random sampling will ensure representation across various clinical stages (I-IV) and molecular typing (Luminal A/B, HER2-positive, triple-negative), enhancing the generalizability of the results. Additionally, a standardized contrast-enhanced ultrasound dynamic tracking protocol will be introduced to monitor changes before and after treatment, and a time-effect association model will be established to verify the predictive efficacy of ultrasound indicators for disease progression and response to targeted therapy.

Conclusion

The contrast-enhanced ultrasound parameters (CEUS) of breast malignant tumors differed significantly from those of benign breast tumors. These differences highlight the diagnostic value of CEUS parameters in clinical breast cancer diagnosis. In addition, CEUS parameters were significantly correlated with the expression of Her-2 and CD147, supporting the use of CEUS for non-invasive early assessment of breast cancer. This provides valuable insight for clinical diagnosis and treatment planning.

Disclosure of conflict of interest

None.

Address correspondence to: Huabin Zhang, Department of Ultrasound, Beijing Tsinghua Changgung Hospital, School of Clinical Medicine, Tsinghua University, No. 168 Litang Road, Changping District, Beijing 102218, PR China. Tel: +86-010-56118892; E-mail: HuabinZh@163.com

References

[1] Ikejima K, Tokioka S, Yagishita K, Kajiura Y, Kanomata N, Yamauchi H, Kurihara Y and Tsunoda H. Clinicopathological and ultrasound characteristics of breast cancer in BRCA1 and BRCA2 mutation carriers. J Med Ultrason (2001) 2023; 50: 213-220.

[2] Wang Y, Li Y, Song Y, Chen C, Wang Z, Li L, Liu M, Liu G, Xu Y, Zhou Y, Sun Q and Shen S. Comparison of ultrasound and mammography for early diagnosis of breast cancer among Chinese women with suspected breast lesions: a prospective trial. Thorac Cancer 2022; 13: 3145-3151.

[3] Tai H, Margolis R, Li J and Hoyt K. H-Scan ultrasound monitoring of breast cancer response to chemotherapy and validation with diffusion-weighted magnetic resonance imaging. J Ultrasound Med 2023; 42: 1297-1306.

[4] Kim YE, Cha JH, Kim HH, Shin HJ, Chae EY and Choi WJ. The accuracy of mammography, ultrasound, and magnetic resonance imaging for the measurement of invasive breast cancer with extensive intraductal components. Clin Breast Cancer 2023; 23: 45-53.

[5] Fei J, Wang GQ, Meng YY, Zhong X, Ma JZ, Sun NN and Chen JJ. Breast cancer subtypes affect the ultrasound performance for axillary lymph node status evaluation after neoadjuvant chemotherapy: a retrospective analysis. Jpn J Clin Oncol 2021; 51: 1509-1514.

[6] Luo WQ, Huang QX, Huang XW, Hu HT, Zeng FQ and Wang W. Predicting breast cancer in breast imaging reporting and data system (BI-RADS) ultrasound category 4 or 5 lesions: a nomogram combining radiomics and BI-RADS. Sci Rep 2019; 9: 11921.

[7] Roca Navarro MJ, Garrido Alonso D, Navarro Monforte Y, García Martínez F, Díaz de Bustamante Durbán T, Córdoba Chicote MV and Oliver Goldaracena JM. Efficacy of ultrasound-guided cryoablation in treating low-risk breast cancer. Radiologia (Engl Ed) 2023; 65: 112-121.

[8] Lee SH and Moon WK. Glandular tissue component on breast ultrasound in dense breasts: a new imaging biomarker for breast cancer risk. Korean J Radiol 2022; 23: 574-580.

[9] Bai X, Wang Y, Song R, Li S, Song Y, Wang H, Tong X, Wei W, Ruan L and Zhao Q. Ultrasound and clinicopathological characteristics of breast cancer for predicting axillary lymph node metastasis. Clin Hemorheol Microcirc 2023; 85: 147-162.

[10] Cui Q, Dai L, Li J, Shen Y, Tao H, Zhou X and Xue J. Contrast-enhanced ultrasound-guided sentinel lymph node biopsy in early-stage breast cancer: a prospective cohort study. World J Surg Oncol 2023; 21: 143.

[11] Chinese Anti-Cancer Association Breast Cancer Committee. Chinese Anti-Cancer Association breast cancer guidelines and standards (2015 edition). Chin J Cancer 2015; 25: 692-754.

[12] Qian X, Pei J, Zheng H, Xie X, Yan L, Zhang H, Han C, Gao X, Zhang H, Zheng W, Sun Q, Lu L and Shung KK. Prospective assessment of breast cancer risk from multimodal multiview ultrasound images via clinically applicable deep learning. Nat Biomed Eng 2021; 5: 522-532.

[13] Baliski C, Jay M and Hamm J. Intraoperative ultrasound is associated with low re-excision rates following breast conserving surgery for non-palpable invasive breast cancers. Am J Surg 2021; 221: 1164-1166.

[14] Marini TJ, Castaneda B, Iyer R, Baran TM, Nemer O, Dozier AM, Parker KJ, Zhao Y, Ser-

ratelli W, Matos G, Ali S, Ghobryal B, Visca A and O'Connell A. Breast ultrasound volume sweep imaging: a new horizon in expanding imaging access for breast cancer detection. J Ultrasound Med 2023; 42: 817-832.

[15] Candelaria RP, Spak DA, Rauch GM, Huo L, Bassett RL, Santiago L, Scoggins ME, Guirguis MS, Patel MM, Whitman GJ, Moulder SL, Thompson AM, Ravenberg EE, White JB, Abuhadra NK, Valero V, Litton J, Adrada BE and Yang WT. BI-RADS ultrasound lexicon descriptors and stromal tumor-infiltrating lymphocytes in triple-negative breast cancer. Acad Radiol 2022; 29 Suppl 1: S35-S41.

[16] Cho E, Lee JH, Park EH and Byun KD. Ultrasound surveillance on detection of nonpalpable supraclavicular recurrence after breast cancer surgery. Med Ultrason 2020; 22: 171-177.

[17] Jabeen K, Khan MA, Alhaisoni M, Tariq U, Zhang YD, Hamza A, Mickus A and Damaševičius R. Breast cancer classification from ultrasound images using probability-based optimal deep learning feature fusion. Sensors (Basel) 2022; 22: 807.

[18] Mo Y, Han C, Liu Y, Liu M, Shi Z, Lin J, Zhao B, Huang C, Qiu B, Cui Y, Wu L, Pan X, Xu Z, Huang X, Li Z, Liu Z, Wang Y and Liang C. HoVer-Trans: anatomy-aware hover-transformer for ROI-free breast cancer diagnosis in ultrasound images. IEEE Trans Med Imaging 2023; 42: 1696-1706.

[19] Sprague BL, Ichikawa L, Eavey J, Lowry KP, Rauscher G, O'Meara ES, Miglioretti DL, Chen S, Lee JM, Stout NK, Mandelblatt JS, Alsheik N, Herschorn SD, Perry H, Weaver DL and Kerlikowske K. Breast cancer risk characteristics of women undergoing whole-breast ultrasound screening versus mammography alone. Cancer 2023; 129: 2456-2468.

[20] Su S, Ray JC, Ooi C and Jain M. Pathology of MRI and second-look ultrasound detected multifocal breast cancer. Acta Oncol 2023; 62: 1840-1845.

[21] Tadesse GF, Tegaw EM and Abdisa EK. Diagnostic performance of mammography and ultrasound in breast cancer: a systematic review and meta-analysis. J Ultrasound 2023; 26: 355-367.

[22] Ferre R, Elst J, Senthilnathan S, Lagree A, Tabbarah S, Lu FI, Sadeghi-Naini A, Tran WT and Curpen B. Machine learning analysis of breast ultrasound to classify triple negative and HER2+ breast cancer subtypes. Breast Dis 2023; 42: 59-66.

[23] Kwon BR, Chang JM, Kim SY, Lee SH, Kim SY, Lee SM, Cho N and Moon WK. Automated breast ultrasound system for breast cancer evaluation: diagnostic performance of the two-view scan technique in women with small breasts. Korean J Radiol 2020; 21: 25-32.

[24] Ferrucci M, Milardi F, Passeri D, Mpungu LF, Francavilla A, Cagol M, Saibene T, Michieletto S, Toffanin M, Del Bianco P, Grossi U and Marchet A. Intraoperative ultrasound-guided conserving surgery for breast cancer: no more time for blind surgery. Ann Surg Oncol 2023; 30: 6201-6214.

[25] Shao Y, Hashemi HS, Gordon P, Warren L, Wang J, Rohling R and Salcudean S. Breast cancer detection using multimodal time series features from ultrasound shear wave absolute vibro-elastography. IEEE J Biomed Health Inform 2022; 26: 704-714.

[26] Yao Z, Luo T, Dong Y, Jia X, Deng Y, Wu G, Zhu Y, Zhang J, Liu J, Yang L, Luo X, Li Z, Xu Y, Hu B, Huang Y, Chang C, Xu J, Luo H, Dong F, Xia X, Wu C, Hu W, Wu G, Li Q, Chen Q, Deng W, Jiang Q, Mou Y, Yan H, Xu X, Yan H, Zhou P, Shao Y, Cui L, He P, Qian L, Liu J, Shi L, Zhao Y, Xu Y, Zhan W, Wang Y, Yu J and Zhou J. Virtual elastography ultrasound via generative adversarial network for breast cancer diagnosis. Nat Commun 2023; 14: 788.

[27] Barth RJ Jr, Krishnaswamy V, Rooney TB, Fox MJ, Burman HEG, Rosenkranz KM, Gass J, Bronfine BI, Angeles CV and Paulsen KD. A pilot multi-institutional study to evaluate the accuracy of a supine MRI based guidance system, the Breast Cancer Locator, in patients with palpable breast cancer. Surg Oncol 2022; 44: 101843.

[28] Hemminki K. Determining the appropriate risk-adapted screening age for familial breast cancer. JAMA Oncol 2020; 6: 933-934.

[29] Catalano O, Fusco R, Carriero S, Tamburrini S and Granata V. Ultrasound findings after breast cancer radiation therapy: cutaneous, pleural, pulmonary, and cardiac changes. Korean J Radiol 2024; 25: 982-991.

[30] Ozler T, Cosar R, Sut N, Nurlu D, Parlar S, Ates S, Dertli MH, Kavuzlu Y, Kavukcu S, Chousein M, Yldz G, Tuncbilek N, Hacoglu MB, Tastekin E and Topalolu S. Comparison of survival between unilateral and bilateral breast cancers using propensity score matching: a retrospective single-center analysis. Breast Cancer Res Treat 2025; 210: 673-686.

[31] Littrup PJ, Mehrmohammadi M and Duric N. Breast tomographic ultrasound: the spectrum from current dense breast cancer screenings to future theranostic treatments. Tomography 2024; 10: 554-573.

[32] Banys-Paluchowski M, Rubio IT, Karadeniz Cakmak G, Esgueva A, Krawczyk N, Paluchowski P, Gruber I, Marx M, Brucker SY, Bündgen N, Kühn T, Rody A, Hanker L and Hahn M. Intraoperative ultrasound-guided excision of non-palpable and palpable breast cancer: systematic

review and meta-analysis. Ultraschall Med 2022; 43: 367-379.
[33] Touzi R, Ben Daly A, Ben Amor A, Ben Dhiab M and Debout C. A descriptive phenomenological study of the women's experiences from the suspicion of breast cancer to the initiation of treatment. Scand J Caring Sci 2025; 39: e70023.
[34] Deng H, Lei J, Jin L and Shi H. Diagnostic efficacy of sentinel lymph node in breast cancer under percutaneous contrast-enhanced ultrasound: an updated meta-analysis. Thorac Cancer 2021; 12: 2849-2856.
[35] Tian L, Wang L, Qin Y and Cai J. Systematic review and meta-analysis of the malignant ultrasound features of triple-negative breast cancer. J Ultrasound Med 2020; 39: 2013-2025.